

Supporting Information for

Synthesis of efficient lanthanides doped glass-ceramic based near-infrared photocatalyst by a complete waterless solid-state reaction method

Experimental Details

The raw materials of CaO(99%), SiO₂ (99%), Al₂O₃(99%), CaF₂(99%), Yb₂O₃ (99.99%), Er₂O₃ (99.99%), were all purchased from Sinopharm chemical Reagent Co. Ltd (China) with analytical grade and they were used as received, nano-anatase TiO₂ (99.9%) for photocatalysis was purchased from Shanghai Titan Scientific Co.Ltd.

The samples were prepared with nominal composition (in mol.%) 43SiO₂-18Al₂O₃-12CaO-24.5CaF₂ -2Yb₂O₃-0.5Er₂O₃ by melt-quenching method. To prepare the mixed samples, all reactants were thoroughly mixed and finely ground prior to the reaction. The raw were completely mixed and crashed in ball crusher (MM400, Germany) for 5min. The well ground stoichiometric chemicals were put into an alumina crucible and melted at 1300 °C for 2 hours, the upconversion precursor glass(UPG) as form after annealed at 400 °C for 2 h and ball milling. Subsequently, the UPG was heat-treated at 650°C for 120 min to form upconversion glass-ceramics (GC650) sample.

Anatase TiO₂ was added according to the molar ratio of CaF₂ in UPG to anatase TiO₂ of 5:1, then crushed and milled adequately in ball crusher (PM100, Germany) for 30min, the mixture was labeled as TUPG. Subsequently, the TUPG was heat-treated at a heating rate of 5°C/min at sintering temperature 650°C for 120min which was labeled as TGC650.

Characterization

The Differential Scanning Calorimetry and Thermogravimetry analyse test (DSC-TG) of the UPG was carried out on a NETSCH STA 449 F3 simultaneous thermal analyzer of German manufacture, and about 15.5±0.5 mg sample placed in an Al₂O₃ ceramic pan was heated from in an fully exposed Ar atmosphere within a temperature range of 25~1200 °C at the heating rates of 10 °Cmin⁻¹. The crystal structures of the samples were identified by X-ray diffraction (XRD) on a Bruker D8 Advance X-ray diffractometer at 40kV and 40 mA using Cu Ka radiation($\lambda= 1.5406 \text{ \AA}$). The morphologies and microstructures were characterized with the Sirion 200 field emission scanning electron microscope (FESEM) equipped with the energy-dispersive spectroscopy (EDS) instrument, and a JEM-2100F transmission electron microscope (TEM) instrument. The particle size was test by using Delsa Nano

particle and zeta potential analyzer (Beckman Coulter, CA, USA). The surface analysis was studied by X-ray photoelectron spectroscopy (XPS, Kratos Axis Ultra DLD), and all the binding energies were calibrated with the C 1s peak at 284.8eV. The absorption spectra were performed on the Lambda 750 UV-vis-NIR spectrophotometer, and the band gap energy was calculated referring to Tauc's formula. Room temperature upconversion fluorescence spectra was measured by a Hitachi F-7000 fluorescence spectrophotometer equipped with a 980 nm semiconductor solid laser with tunable power, and the photoluminescence (PL) spectra, was measured by a Hitachi F-7000 fluorescence spectrophotometer at 300nm.

Measurement of Photocatalytic Activities

The photocatalytic activities of the samples were evaluated by the decomposition of MO under the NIR light (≥ 780 nm) irradiations (provided by 500 W Xenon lamp). 20 mg of the samples were added in the MO aqueous solutions (10 mg/L, 20 mL). Before irradiation, the mixtures were kept in the dark with magnetic stirring for 2 h to establish an adsorption/desorption equilibrium. Every 30 min intervals, 1.5 mL of the mixtures were collected and centrifuged. The changed absorption peak intensities of supernatant at 464 nm were detected by a UV-vis spectrophotometer (Hitachi U-3900).

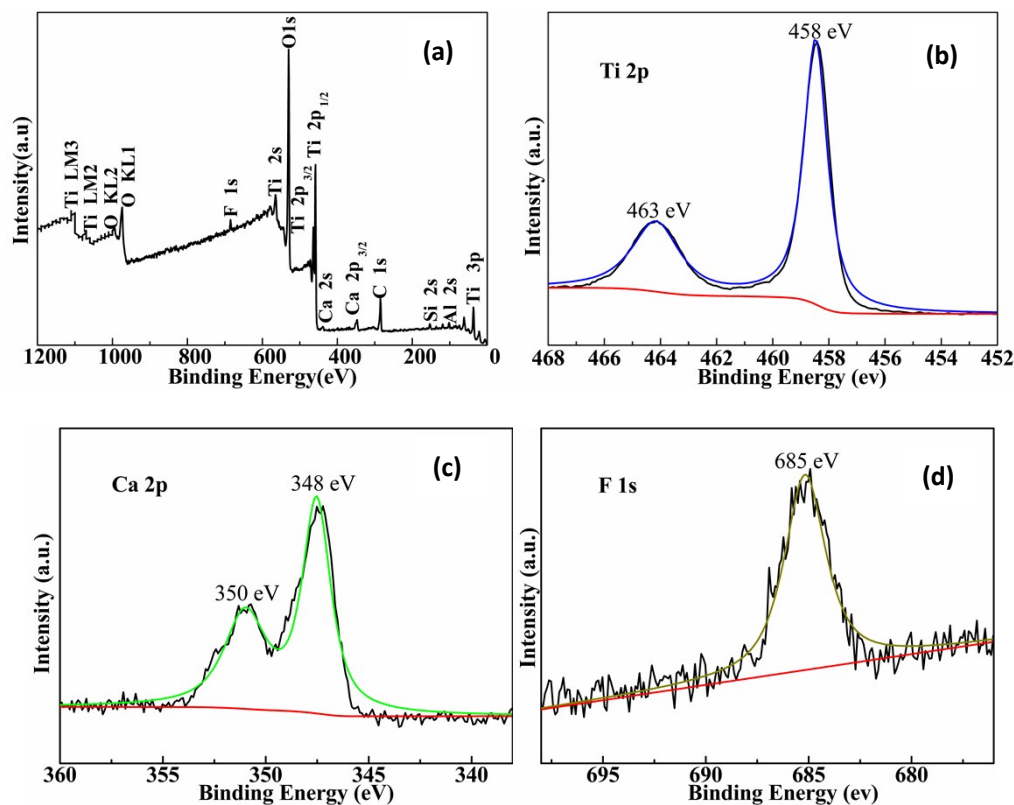


Figure S1. XPS spectra of TGC650: (a) survey scan, (b) Ti 2p, (c) Ca 2p, and (d) F 1s.

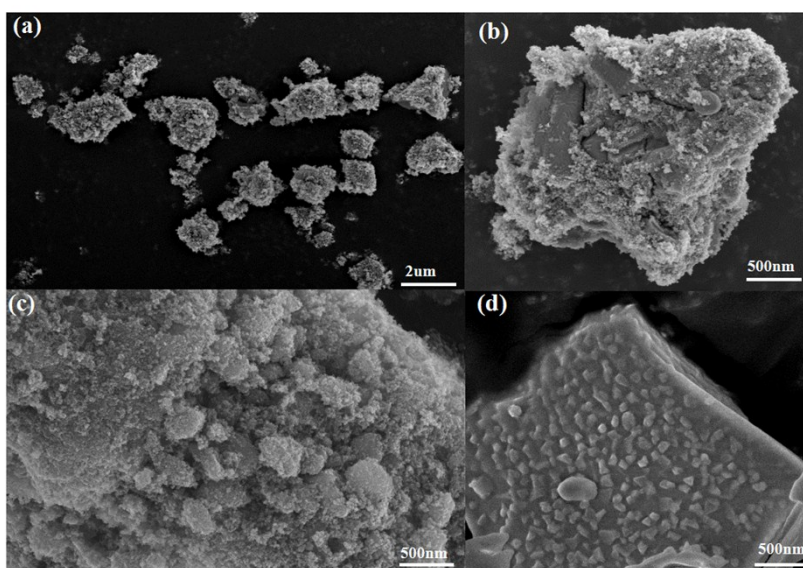


Figure S2. SEM images of (a)-(c) TGC650 and (d) GC650.

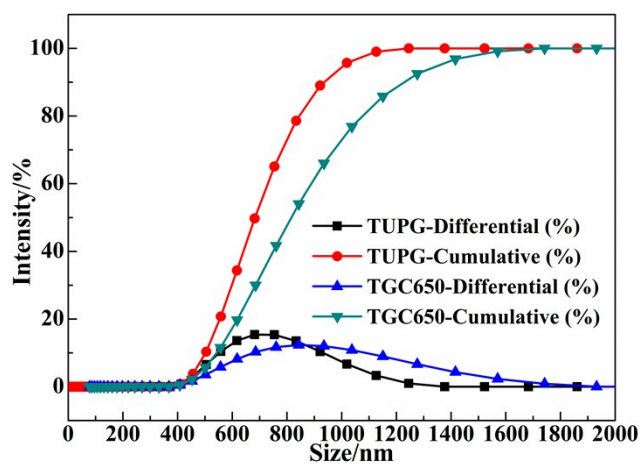


Figure S3. Sizes of TGC650 and TUPG

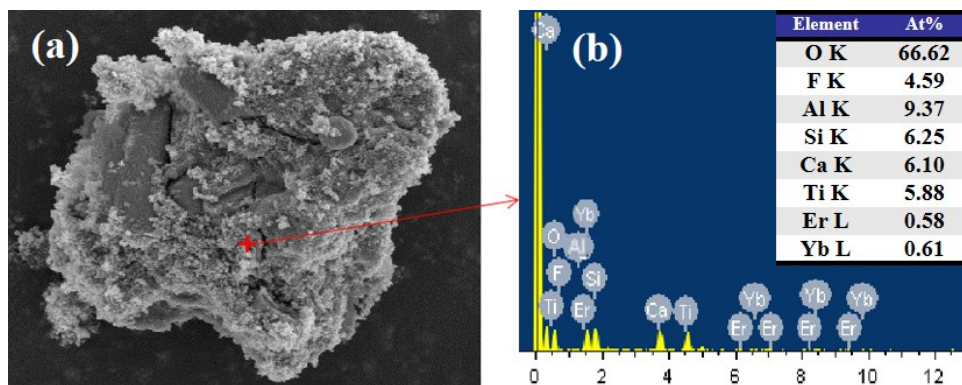


Figure S4. (a) SEM and (b) EDS of TGC650

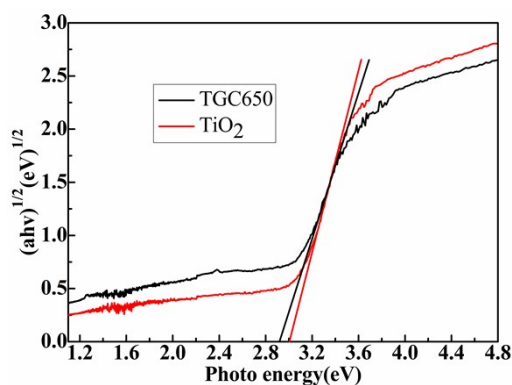


Figure S5. The plots of the $(ah\nu)^{1/2}$ versus photon energy ($h\nu$) for TGC650 and pure TiO_2 .

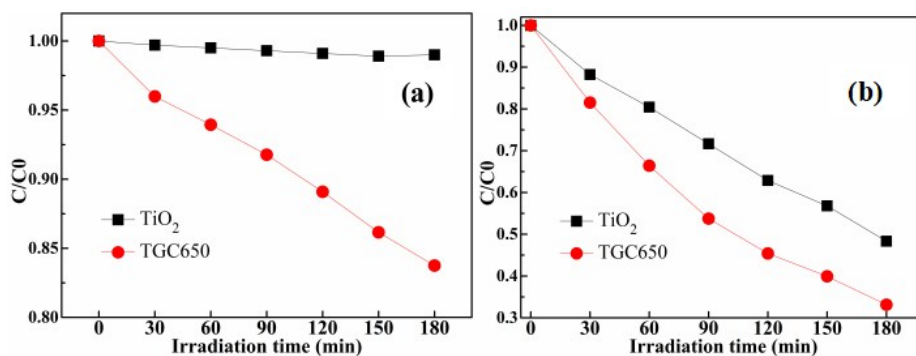


Figure S6. (a) C/C_0 conversion plots of salicylic acid for pure TiO_2 and TGC650 under NIR light ($\lambda \geq 780\text{nm}$) irradiation. (b) C/C_0 conversion plots of salicylic acid for pure TiO_2 and TGC650 under UV-vis-NIR light irradiation.

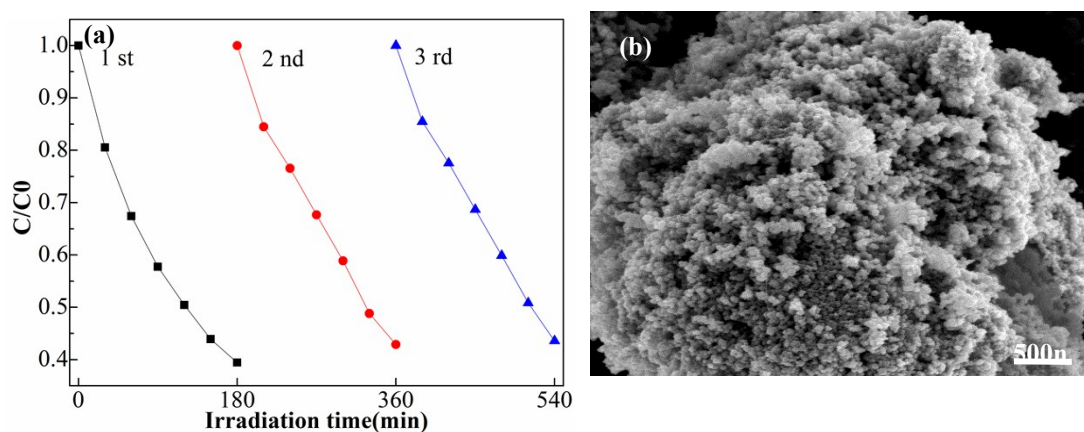


Figure S7. (a) Recycling photocatalytic degradation of MO over TGC650 under xenon lamp irradiation, (b) the corresponding SEM image of TGC after the 3th run under xenon lamp irradiation

Table. S1 Photodegradation performances of NIR photocatalysts

Photocatalyst	Absorption Edge	Pollutant and Concentration	Time and efficiency	Reaction condition	Ref.
TiO ₂ /GC	425 nm	MO, 10mg/L	3 h, 13 %	1000 W, >780nm	In this paper
Er ³⁺ /Tm ³⁺ /Yb-CaF ₂ /BiVO ₄	506 nm	MO, 10mg/L	6 h, 10 %	1W 980 nm laser	[1]
YF ₃ : Yb, Tm/TiO ₂	-	MB, 10mg/L	30 h, 70 %	1.5 W 980 nm laser	[2]
NaYF ₄ :Yb/Tm@TiO ₂	387 nm	MO (15/0.5)	24 h, 69 %	1W 980 nm laser	[3]
Er ³⁺ /Yb ³⁺ -(CaF ₂ /TiO ₂)	425 nm	MO, 10mg/L	3 h, about 7 %	1000 W, >780nm	[4]

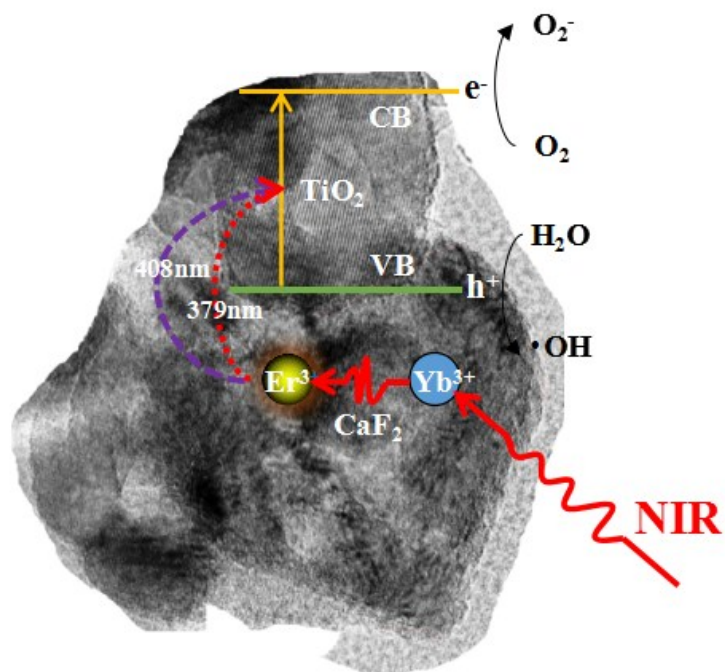


Figure S8. The energy transfer mechanism for NIR-driven photocatalytic degradation.

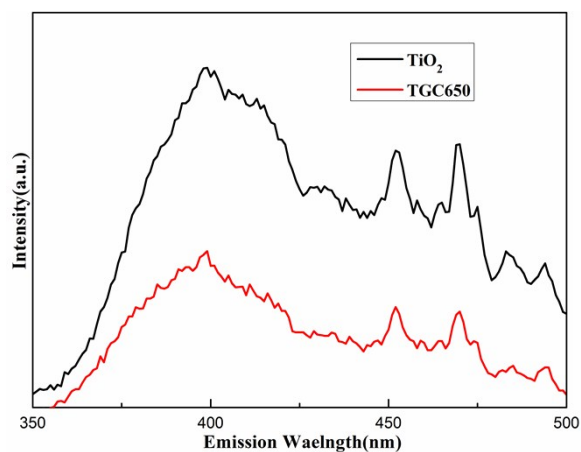


Figure S9. PL emission spectra excited of the TiO₂ and TGC650 samples at 300nm at room temperature

References:

- [1]. Huang S. , et al., *Nanoscale*, 2014, **6**, 1362.
- [2]. Guo X, Di W, Chen C, et al. [J]. *Dalt. Tran.* , 2014, **43**, 1048.
- [3]. Xu D. , Lian Z., Fu M., et al. *Appl. Cata. B*, 2013, **142**, 377.
- [4]. Huang S, Lou Z, Shan A, et al. *J. Mater. C. A*, 2014, **2**, 16165.